Assembly and Signaling of CRLR and RAMP1 Complexes Assessed by BRET[†]

Madeleine Héroux, Billy Breton, Mireille Hogue, and Michel Bouvier*

Département de Biochimie, Institut de Recherche en Immunologie et Cancérologie and Groupe de Recherche Universitaire sur le Médicament, Université de Montréal, C.P. 6128, Succursale Centre-Ville, Montréal, QC, Canada H3C 3J7

Received October 30, 2006; Revised Manuscript Received April 5, 2007

ABSTRACT: Biochemical and functional evidence suggest that the calcitonin receptor-like receptor (CRLR) interacts with receptor activity-modifying protein-1 (RAMP1) to generate a calcitonin gene-related peptide (CGRP) receptor. Using bioluminescence resonance energy transfer (BRET), we investigated the oligomeric assembly of the CRLR−RAMP1 signaling complex in living cells. As for their wild-type counterparts, fusion proteins linking CRLR and RAMP1 to the energy donor *Renilla* luciferase (*R*luc) and energy acceptor green fluorescent protein (GFP) reach the cell surface only upon coexpression of CRLR and RAMP1. Radioligand binding and cAMP production assays also confirmed that the fusion proteins retained normal functional properties. BRET titration experiments revealed that CRLR and RAMP1 associate selectively to form heterodimers. This association was preserved for a mutated RAMP1 that cannot reach the cell surface, even in the presence of CRLR, indicating that the deficient targeting resulted from the altered conformation of the complex rather than a lack of heterodimerization. BRET analysis also showed that, in addition to associate with one another, both CRLR and RAMP1 can form homodimers. The homodimerization of the coreceptor was further confirmed by the ability of RAMP1 to prevent cell surface targeting of a truncated RAMP1 that normally exhibits receptor-independent plasma membrane delivery. Although the role of such dimerization remains unknown, BRET experiments clearly demonstrated that CRLR can engage signaling partners, such as G proteins and β-arrestin, following CGRP stimulation, only in the presence of RAMP1. In addition to shed new light on the CRLR−RAMP1 signaling complex, the BRET assays developed herein offer new biosensors for probing CGRP receptor activity.

The discovery in 1998 by McLatchie et al. of a new family of proteins named receptor activity-modifying proteins (RAMPs)[1] challenged the traditional views of how G protein-coupled receptors (GPCRs) function (*1*). These proteins were first shown to promote the maturation and transport, and to define the pharmacological properties of an orphan receptor, the calcitonin receptor-like receptor (CRLR). Three RAMPs were identified (RAMP1, RAMP2, and RAMP3), forming a small family of single-transmembrane domain proteins that share the same topological organization but only 30% identical sequence. When associated with RAMP1, CRLR functions as a calcitonin gene-related peptide (CGRP) receptor, while it acts as an adrenomedullin (AM) receptor when coexpressed with RAMP2 or RAMP3. Taken with biochemical evidence suggesting physical interactions between RAMPs and CRLR (*2*−*9*), the observation that radiolabeled ligands could be cross-linked to both RAMPs and CRLR (*1*−*4*, *10*, *11*) clearly indicated that RAMPs act as genuine coreceptors of CRLR. In addition to the family B seven-transmembrane domain receptor (7TMR) CRLR, several members of this same family [calcitonin (*12*), glucagon, vasoactive intestinal polypeptide/pituitary adenylate cyclase-activating peptide 1, and parathyroid hormone 1 and 2 receptors (*13*)] and one member of family C 7TMR [calcium-sensing receptor (*14*)] were found to interact with RAMPs. In several instances, interactions between RAMPs and 7TMR were found to affect their cellular trafficking. In the case of CRLR and RAMP1, the coexpression of the two proteins is essential for their common cell surface targeting. When expressed alone, CRLR is retained in the endoplasmic reticulum (ER), whereas RAMP1 is found in the ER and the Golgi (*6*) as a consequence of a four-residue retention motif (SKRT) in its C-terminal tail (*4*).

Despite the strong evidence suggesting that 7TMR−RAMP complexes can form functional units that are involved in both receptor trafficking and signaling, almost no information concerning the formation of these complexes and their interactions with other signaling partners in living cells is available. Similarly, very little is known about the RAMP-associated 7TMR in the context of another emerging concept in GPCR trafficking and signaling, receptor dimerization.

[†] This work was supported by a grant from the Canadian Institute for Health Research (M.B.). M. Héroux holds a studentship from the Canadian Institute for Health Research. M.B. holds a Canada Research Chair in Signal Transduction and Molecular Pharmacology.

* To whom correspondence should be addressed: Institut de Recherche en Immunologie et Cancérologie, Université de Montréal, C.P. 6128, Succursale Centre-Ville, Montréal, QC, Canada H3C 3J7. Telephone: (514) 343-6319. Fax: (514) 343-7780. E-mail: michel.bouvier@umontreal.ca.

[1] Abbreviations: 7TMR, seven-transmembrane domain receptor; AM, adrenomedullin; BRET, bioluminescence resonance energy transfer; CGRP, calcitonin gene-related peptide; CRLR, calcitonin receptor-like receptor; DMEM, Dulbecco's modified Eagle's medium; ER, endoplasmic reticulum; Fz, Frizzled; GFP, green fluorescent protein; GPCR, G protein-coupled receptor; Gs, stimulatory G protein; HEK, human embryonic kidney; HRP, horseradish peroxidase; LRP6, low-density lipoprotein receptor-related protein 6; RAMP, receptor activity-modifying protein; *R*luc, *Renilla* luciferase; WT, wild-type.

10.1021/bi0622470 CCC: $37.00
Published on Web 05/16/2007

Indeed, a growing body of evidence indicates that many GPCRs can exist as homo- or heterodimers between closely related 7TMR subtypes, a process also believed to be involved in receptor trafficking and pharmacological diversity (*15*). Whether a 7TMR such as CRLR, which requires RAMPs for cell surface targeting and signaling, can also form homodimers remains an open question. Interestingly, indirect biochemical evidence suggests that RAMP1 and RAMP3 can also form homodimers (*1*, *6*, *16*, *17*). Once again, however, the oligomeric status of these proteins has not been explored in living cells.

This study was therefore undertaken to further investigate the oligomeric status of CRLR and RAMP1, and their interaction with signaling partners in intact cells using bioluminescence resonance energy transfer (BRET). Our results demonstrate that, in addition to interacting with one another, CRLR and RAMP1 can both form homodimers. Despite the formation of CRLR homodimers, the coexpression of RAMP1 was essential for allowing agonist-promoted interaction between the 7TMR and either G proteins or β-arrestin, confirming the essential role of the CRLR−RAMP complex in signal transduction.

EXPERIMENTAL PROCEDURES

Materials

Dulbecco's modified Eagle's medium (DMEM), fetal bovine serum, glutamine, penicillin, and streptomycin were all from Wisent (St. Bruno, QC). [^{125}I]CGRP and [^{125}I]AM (specific activity of 2000 Ci/mmol) were from GE Healthcare Life Sciences (Little Chalfont, U.K.), and human αCGRP and AM were from Bachem AG (Bubendorf, Switzerland). Mouse anti-myc antibodies (9E10 clone) were produced by our core facility as ascite fluids. Texas Red-conjugated secondary antibodies and rabbit anti-HA antibodies were obtained from Santa Cruz Biotechnology (Santa Cruz, CA). Immobilized anti-HA rat antibodies were from Roche Molecular Biochemicals (Laval, QC), and rabbit anti-myc antibodies were from Sigma (St. Louis, MO). Horseradish peroxidase (HRP)-conjugated secondary antibodies were purchased from GE Healthcare Life Sciences. *O*-Phenylenediamine dihydrochloride tablets (HRP substrate) were from Sigma. The chemiluminescence kit was from Perkin-Elmer Life Sciences (Boston, MA). DeepBlue coelenterazine was purchased from Perkin-Elmer Life Sciences (Woodbridge, ON) and coelenterazine H from Molecular Probes (Burlington, ON).

Expression Vectors

RAMP1, myc-RAMP1, CRLR, myc-CRLR, and HA-CRLR. Human cDNAs encoding RAMP1, myc-RAMP1, CRLR, myc-CRLR, and HA-CRLR were subcloned into the pcDNA3 expression plasmid as previously described (*1*) and were graciously provided by S. M. Foord (GlaxoSmithKline).

myc-RAMP1-Rluc, myc-RAMP1-GFP, myc-CRLR-Rluc, and myc-CRLR-GFP [where Rluc stands for Renilla luciferase and GFP for green fluorescent protein 10 (18)]. The coding sequences of myc-RAMP1 and myc-CRLR were amplified by PCR to generate stop codon-free fragments that were subcloned into pcDNA3.1 zeo (+). The *R*luc or GFP fragments were then inserted in-frame 3′ of the RAMP1 and CRLR, creating a six-amino acid linker between the proteins.

Fz1-GFP and LRP6-GFP (where Fz1 stands for rat Frizzled 1 and LRP6 for human low-density lipoprotein receptor-related protein 6). These vectors were generously provided by R. T. Moon (University of Washington School of Medicine, Seattle, WA) and were constructed by incorporating the GFP coding sequence (from pGFP2 N1, Perkin-Elmer) in-frame 3′ of the LRP6 and Fz1 sequence.

myc-RAMP1C104A-GFP. The RAMP1 mutant was constructed by PCR site-directed mutagenesis, replacing cysteine 104 with alanine using myc-RAMP1-GFP as a template.

RAMP2-GFP and RAMP3-GFP. These constructs were generously provided by P. M. Sexton (Monash University, Clayton, Australia) and were constructed using the Gateway system technology (Invitrogen). RAMP2 and RAMP3 were incorporated into the pENTER vector and then, via a recombination reaction, cloned into the pGFP2 destination vector, creating a linker of 30 amino acids between the RAMP and the GFP.

myc-RAMP1Δ8-GFP. A PCR fragment lacking the stop codon plus the last eight amino acids from the C-terminus (SKRTEGIV) was generated using myc-RAMP1 as a template. This fragment was subcloned into pcDNA3.1 zeo (+) and the GFP fragment inserted in-frame 3′ of RAMP1Δ8, creating a six-amino acid linker between the two proteins.

HA-RAMP1-Rluc. The myc epitope at the N-terminus of myc-RAMP1-*R*luc described above was replaced with the HA epitope cut out from the HA-CRLR construct, also described above.

$G\gamma_2$-Rluc and β-Arrestin2-Rluc (where $G\gamma_2$ stands for the G protein γ_2 subunit). The coding sequences of $G\gamma_2$ and rat β-arrestin2 were inserted in-frame 5′ of the *R*luc sequence as previously described (*19*, *20*).

All constructs were confirmed by sequencing.

Cell Culture and Transfections

Human embryonic kidney 293T (HEK293T) cells were maintained in DMEM supplemented with 10% (v/v) fetal bovine serum, 2 mM glutamine, 100 units/mL penicillin, and 100 μg/mL streptomycin at 37 °C in a humidified atmosphere of 95% air and 5% CO_2. Transient transfections were performed using the calcium phosphate precipitation method (*21*), except for the agonist-induced BRET experiments between CRLR and both Gγ and β-arrestin for which transfections were performed using polyethyleneimine as the transfecting agent (*22*). In all cases, the amount of DNAs between conditions was kept constant by adding the appropriate amount of empty vectors. All experiments were carried out 48 h after transfection.

Immunofluorescence Microscopy

Labeling of Permeabilized Cells. Transfected cells were fixed with PBS containing 3% (w/v) paraformaldehyde for 15 min and permeabilized with 0.25% Triton X-100 in blocking buffer [PBS containing 0.2% (w/v) BSA] at room temperature for 15 min. Cells were then incubated with anti-myc (9E10) antibodies (1/100 dilution) for 30 min. After three washes in blocking buffer, anti-mouse Texas Red-conjugated antibodies (1/500 dilution) were added for 30 min. The samples were then extensively washed, mounted onto slides using Airvol mounting medium, and analyzed by

confocal laser-scanning microscopy using a Leica TCS SP1 confocal microscope.

Cell Surface Labeling. Transfected cells were incubated in blocking buffer, and anti-myc (9E10) antibodies (1/100 dilution) were added for 1 h on ice. Cells were then washed and fixed with PBS containing 3% (w/v) paraformaldehyde for 15 min, treated with the appropriate secondary antibodies, and analyzed as described above.

Accumulation of cAMP

cAMP accumulation was assessed using the CatchPoint cAMP fluorescent assay kit from Molecular Devices. Briefly, cells were detached and resuspended in stimulation buffer [PBS containing 0.2% (w/v) EDTA, 0.1% (w/v) glucose, and 0.75 mM 3-isobutyl-1-methylxanthine]. Cells were then distributed in 96-well plates and incubated with the indicated concentrations of CGRP. The reaction was stopped, and lysates were transferred to 384-well plates coated with goat anti-rabbit antibodies. Rabbit anti-cAMP antibodies were added, followed by HRP-conjugated cAMP. After 2 h, the plates were extensively washed, the Stoplight Red substrate was added, and the plates were read using a FlexStation (Molecular Devices). cAMP accumulation experiments were performed in triplicate.

Radioligand Binding

Transfected HEK293T cells, seeded in 24-well plates, were washed three times with cold PBS and incubated on ice for 3 h in binding buffer [DMEM containing 0.2% (w/v) BSA and 20 mM HEPES (pH 7.4)] with 200 pM [^{125}I]CGRP or [^{125}I]AM, in the absence (total binding) or presence of increasing concentrations of unlabeled ligand. Nonspecific binding was defined as binding in the presence of 1 μM unlabeled CGRP or AM. After being incubated, cells were washed once with binding buffer and twice with PBS and then solubilized with 0.5 M NaOH. The associated cellular radioactivity was measured in a γ-counter. Binding experiments were performed in triplicate.

BRET^2

Cells were washed twice with PBS, detached, and resuspended in PBS containing 0.1% (w/v) glucose. Cells were then distributed in 96-well plates (100 000 cells/well) (white plates from Corning #3912), and DeepBlue coelenterazine was added at a final concentration of 5 μM. Readings were collected using a modified TopCount apparatus (Packard Bioscience) that allows the sequential integration of the signals detected in the 370−450 and 500−530 nm ranges. The BRET signal corresponds to the ratio of the light emitted by GFP (500−530 nm) over the light emitted by *R*luc (370−450 nm). The values were corrected by subtracting the BRET background signal detected when *R*luc constructs were expressed alone. For BRET titration curve experiments, cells were transfected with a constant amount of *R*luc construct and increasing quantities of GFP construct. The total luminescence and fluorescence were measured to control for relative expression levels of donor and acceptor proteins, respectively. BRET values were then plotted as a function of the total fluorescence/luminescence ratios (GFP/*R*luc) and the curves fitted using nonlinear or linear least-squares regression functions (GrapPad Prism) (*18*). To assess the effect of CGRP on the BRET signal between myc-CRLR-*R*luc and myc-RAMP1-GFP, membranes were prepared from HEK293T cells expressing these two constructs. Cells were mechanically detached in membrane buffer [75 mM Tris (pH 7.4), 5 mM EDTA, 12.5 mM $MgCl_2$, 10 μg/mL benzamidine, 5 μg/mL soybean trypsin inhibitor, and 5 μg/mL leupeptin], followed by lysis at 4 °C using a polytron. Nucleus and large cellular debris were eliminated by centrifugation at 100*g* for 5 min at 4 °C. The supernatant was then centrifuged at 44000*g* for 20 min at 4 °C. The pelleted membranes were washed twice in membrane buffer and finally resuspended in an appropriate volume of membrane buffer. For agonist-induced BRET experiments, cells (100 000 cells/well) or membrane preparations (3−27 μg of protein/well) were distributed in 96-well plates and treated with the indicated concentrations of CGRP for 10 min at room temperature before DeepBlue coelenterazine was added. BRET readings were then collected at room temperature as described above, immediately following addition of DeepBlue coelenterazine.

Total Luminescence Measurement

Because BRET experiments lead to the transfer of a fraction of the luciferase-emitted energy to the GFP partner, the amount of light detected in the channel corresponding to the *R*luc emission upon addition of DeepBlue coelenterazine is diminished in proportion to the extent of energy transfer. To accurately determine the amount of *R*luc fusion protein expressed under each condition, the total luminescence was measured following the addition of coelenterazine H, a luciferase substrate that leads to luminescence emission at a wavelength that does not allow the transfer of energy to GFP. Briefly, transfected HEK293T cells resuspended in PBS with 0.1% (w/v) glucose were distributed in 96-well plates (100 000 cells/well) (clear bottom plates from Corning #3632), and coelenterazine H was added at a final concentration of 5 μM. The total luminescence generated by *R*luc constructs was determined using a LumiCount (Packard Bioscience), 10 min after the addition of coelenterazine H. This measurement was performed on a fraction of the cell used for BRET or quantitative ELISA experiments.

Total Fluorescence Measurement

The amount of GFP-fused protein expressed was assessed by measuring the total fluorescence upon direct light excitation of the fluorophore. Briefly, transfected HEK293T cells resuspended in PBS with 0.1% (w/v) glucose were distributed in 96-well plates (100 000 cells/well) (clear bottom plates from Corning #3632), and the total fluorescence emitted by GFP constructs was measured using a FluoroCount (Packard Bioscience) with excitation and emission filters set at 400 and 510 nm, respectively. The values were corrected by subtracting the background signal detected in cells transfected with the empty vector instead of GFP constructs. These measurements were performed on a fraction of the cell used for BRET or quantitative ELISA experiments.

Co-Immunoprecipitation

Transfected cells were washed twice with PBS, lysed for 1 h at 4 °C in lysis buffer [50 mM Tris (pH 7.4), 150 mM NaCl, 1% (v/v) Nonidet P-40, 0.5% (w/v) sodium deoxycholate, 50 mM iodoacetamide, 10 μg/mL benzamidine, 5

μg/mL soybean trypsin inhibitor, and 5 μg/mL leupeptin], and centrifuged at 150000*g* for 1 h at 4 °C to remove unsolubilized material. The protein concentration of the lysates was determined, and the same quantity of total proteins was used in each immunoprecipitation reaction. Lysates were incubated overnight at 4 °C with immobilized anti-HA rat antibodies. Antibody−antigen complexes were collected by centrifugation and successively washed four times with cold lysis buffer containing 150, 250, 350, and finally 150 mM NaCl. The final pellet was resuspended in sample buffer containing 60 mM Tris (pH 6.8), 2% (w/v) SDS, 4.5 M urea, and 100 mM dithiothreitol. Protein samples were resolved by 8% SDS−polyacrylamide gel electrophoresis, transferred to nitrocellulose, and subjected to immunoblotting using rabbit anti-myc antibodies (1/1000 dilution) or rabbit anti-HA antibodies (1/10000 dilution).

Quantitative Measurement of Cell Surface RAMPs

Forty-eight hours post-transfection, cells were washed twice, fixed with PBS containing 3% (w/v) paraformaldehyde, and incubated in blocking buffer [PBS containing 0.2% (w/v) BSA] for 15 min. Anti-myc (9E10) antibodies (1/500 dilution) were added for 30 min. After three washes in blocking buffer, anti-mouse HRP-conjugated antibodies (1/500 dilution) were added for 30 min. Cells were then extensively washed, and immunoreactivity was revealed by the addition of the HRP substrate according to the manufacturer's instructions. For each ELISA experiment, a mock condition corresponding to cells transfected with the empty vector was included, and the values obtained for the different conditions were corrected by dividing the background signal detected from the mock condition. Triplicates were performed for each condition within an ELISA experiment. The amount of cell surface myc-RAMP1-GFP, myc-RAMP1Δ8-GFP, or myc-RAMP1C104A-GFP obtained with the ELISA was plotted as a function of its total expression level, assessed by measuring the total fluorescence (as described in the previous section). The relative amount of HA-RAMP1-*R*luc coexpressed with myc-RAMP1Δ8-GFP was also assessed by measuring the total luminescence.

RESULTS AND DISCUSSION

Characterization of Rluc- and GFP-Fused CRLR and RAMP1. To gain insight into the assembly of CRLR−RAMP1 signaling complexes, a "noninvasive" proximity-based assay exploiting the nonradiative transfer of energy between luciferase and GFP (BRET) was used. For this purpose, fusion proteins were generated in which the energy donor *R*luc or the energy acceptor GFP was fused at the carboxyl terminus of either myc-CRLR or myc-RAMP1. To confirm that these fusion proteins behaved like their wild-type (WT) counterparts, we first studied their subcellular localization using confocal immunofluorescence microscopy. As shown in Figure 1, in the absence of cotransfected RAMP1, myc-CRLR-*R*luc and myc-CRLR-GFP were largely retained intracellularly. The weak cell surface immunofluorescence detected for both myc-CRLR-*R*luc and myc-CRLR-GFP most likely resulted from a low level of endogenous RAMP in these cells (ref *1* and see also below) and not from the presence of *R*luc or GFP fused to the carboxyl terminus of myc-CRLR since a similar weak cell surface expression

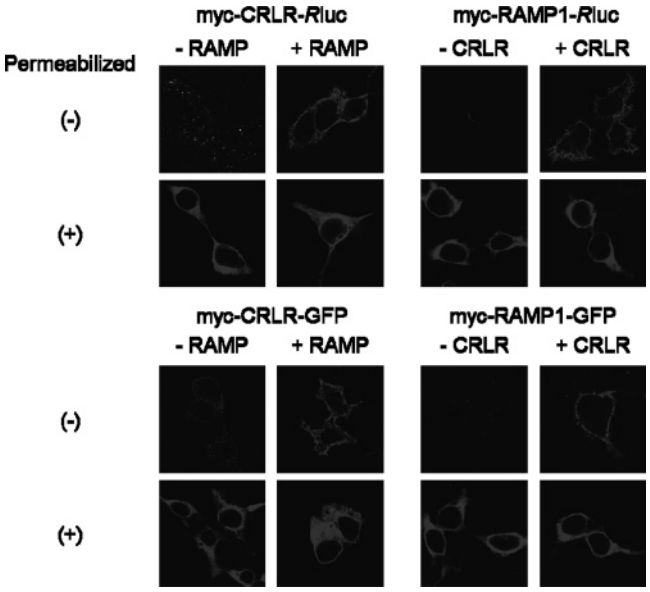

FIGURE 1: Cell surface targeting of *R*luc- and GFP-fused CRLR and RAMP1. HEK293T cells were transfected with myc-CRLR-*R*luc, myc-CRLR-GFP, myc-RAMP1-*R*luc, or myc-RAMP1-GFP, alone or in combination with RAMP1 (in the case of myc-CRLR-*R*luc and myc-CRLR-GFP), or CRLR (in the case of myc-RAMP1-*R*luc and myc-RAMP1-GFP). Cellular localization of the fusion proteins was assessed by immunofluorescence confocal microscopy in intact (−) or permeabilized (+) cells, using anti-myc antibodies and Texas Red-conjugated secondary antibodies. The figures are representative of two independent experiments.

was also observed for the myc-CRLR construct without carboxyl-terminally fused *R*luc or GFP (Figure S1 of the Supporting Information). In the absence of CRLR, myc-RAMP1-*R*luc and myc-RAMP1-GFP were restricted to the inside of the cells (Figure 1). As is the case for their WT counterparts (*1*, *6*), the intracellular retention of the four fusion constructs transfected alone can be easily appreciated by the strong immunofluorescence signals observed after cell permeabilization. A clearly distinct distribution pattern was observed when the CRLR and RAMP1 constructs were coexpressed. Indeed, cell surface expression of both myc-CRLR-*R*luc and myc-CRLR-GFP was greatly enhanced by the cotransfection of RAMP1. Likewise, myc-RAMP1-*R*luc and myc-RAMP1-GFP were clearly detected at the cell surface upon coexpression of CRLR. These results demonstrate that the addition of either *R*luc or GFP did not affect the normal distribution pattern of CRLR and RAMP1, each fusion protein requiring the coexpression of their respective partner for efficient cell surface targeting, in agreement with previous reports on the WT proteins (*1*, *6*).

Next, we wanted to assess the functionality of the four fusion proteins (-*R*luc and -GFP) by testing their ability to promote accumulation of cAMP upon agonist stimulation. First, the functionality of myc-CRLR-*R*luc and myc-CRLR-GFP was tested in cells cotransfected with RAMP1. As seen in Figure 2A, CGRP-induced cAMP production was observed in cells transfected with RAMP1 alone. However, coexpression of either CRLR, myc-CRLR-*R*luc, or myc-CRLR-GFP led to a major increase in both the efficacy and potency of CGRP. The EC_{50} and the maximal responses generated upon expression of either of the two fusion proteins (myc-CRLR-*R*luc or myc-CRLR-GFP) were comparable to those obtained with the WT CRLR, indicating that the

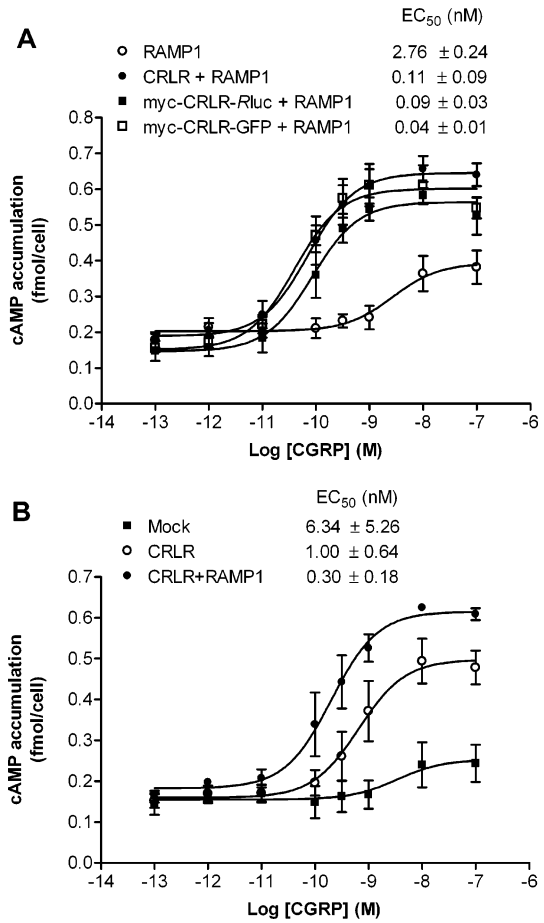

FIGURE 2: Signaling properties of *R*luc- and GFP-fused CRLR. HEK293T cells transfected with the empty vector (mock) or the indicated plasmids were stimulated with increasing concentrations of CGRP, and the cAMP production was assessed. The curves shown represent the mean ± standard error of the mean of three independent experiments.

addition of the myc, *R*luc, or GFP tags to CRLR did not affect the Gs coupling potential of the receptor.

The cAMP production obtained in cells transfected with RAMP1 alone most likely reflects the presence of low levels of endogenous receptor that can bind CGRP and activate adenylyl cyclase upon interaction with RAMP. Since low levels of endogenous RAMP proteins are also present in HEK293T cells (*1*), one would suspect that we should be able to observe cAMP production in nontransfected cells. Indeed, cells transfected with an empty vector conferred a small but measurable CGRP-promoted adenylyl cyclase activity (Figure 2B). Interestingly, the cotransfection of CRLR and RAMP1 not only resulted in an increase in the level of maximal CGRP-stimulated cAMP production when compared with untransfected or RAMP1 transfected cells but also led to an increase in CGRP potency. This decrease in CGRP EC_{50} may reflect the generation of spare receptor (i.e., more receptor than the amount required to maximally stimulate the adenylyl cyclase activity even at a subsaturating concentration of agonist, leading to a leftward shift in the concentration−response curve). This possibility is supported by the observation that the EC_{50} of CGRP for activation of the adenylyl cyclase is smaller than its IC_{50} derived from a radioligand binding assay (see below).

When we sought to test the functionality of the RAMP1 constructs, it was noted that, as expected from the presence of endogenous RAMP, transfection of CRLR alone was sufficient to confer a sizable cAMP accumulation response, rendering it difficult to assess the functionality of the RAMP1 fusion constructs using this second-messenger generation assay. Indeed, although cotransfection of CRLR with RAMP1 tended to increase both the efficacy and the potency of CGRP in activating adenylyl cyclase activity (Figure 2B), the differences were too small to allow reliable assessment of the RAMP1 fusion proteins. To circumvent this technical problem, we turned to a radioligand binding assay. Indeed, the lack of signal amplification characteristic of radioligand binding assays contrasts with the high level of amplification of second-messenger generation techniques and greatly reduces the impact of the endogenous RAMP on the readout. In cells transfected with CRLR alone, only marginal [^{125}I]-CGRP binding could be detected. In contrast, cotransfection of either WT-RAMP1, myc-RAMP1-*R*luc, or myc-RAMP1-GFP conferred greater [^{125}I]CGRP binding, which could be displaced with high affinity by nonlabeled CGRP (Table 1). Identical IC_{50} values were obtained for WT RAMP1 and myc-RAMP1-GFP, whereas a slightly higher apparent affinity was observed for myc-RAMP1-*R*luc. The maximal binding observed upon transfection of the different RAMP1 fusion proteins was somewhat lower than that obtained with WT RAMP1. This difference, which is particularly evident for myc-RAMP1-*R*luc, most likely reflects different expression levels rather than altered binding properties, since the apparent affinities of CGRP (IC_{50} values) observed were at least as high as that obtained for WT RAMP1. Taken with the observation that myc-RAMP1-*R*luc and myc-RAMP1-GFP have the same cell surface targeting pattern as WT RAMP1 (Figure 1), the binding data indicate that the fusion of *R*luc or GFP did not promote major changes in RAMP1 functionality.

Table 1: Binding Properties of *R*luc- and GFP-Fused RAMP1

DNA construct	specific [^{125}I]CGRP binding (fmol/well)	IC_{50} (nM)
CRLR	0.12 ± 0.06	2.4 ± 0.8[a]
CRLR−RAMP1	2.45 ± 0.19	28.6 ± 6.7[b]
CRLR−myc-RAMP1-*R*luc	0.24 ± 0.04	4.6 ± 1.6[a]
CRLR−myc-RAMP1-GFP	1.35 ± 0.38	25.7 ± 13.7[b]
CRLR−myc-RAMP1Δ8-GFP	1.32 ± 0.27	7.1 ± 1.6[b]

[a] Values are expressed as the mean ± standard deviation calculated from two independent experiments. [b] Values are expressed as the mean ± standard error of the mean calculated from three to four independent experiments. Specific binding was assessed by subtracting the amount of [^{125}I]CGRP binding obtained in the absence and presence of unlabeled 1 μM CGRP. IC_{50} corresponds to the concentrations of unlabeled CGRP inhibiting 50% of the [^{125}I]CGRP binding. [^{125}I]CGRP was used at a tracer concentration of 200 pM. Conditions were selected such that the amount of receptor-bound radioligand was negligible (<6%) compared to the total amount of [^{125}I]CGRP added (i.e., free ligand concentration ≈ total ligand concentration added). Specific binding represented 45% (CRLR alone), 93% (CRLR−RAMP1), 61% (CRLR−myc-RAMP1-*R*luc), 89% (CRLR−myc-RAMP1-GFP), and 94% (CRLR−myc-RAMP1Δ8-GFP) of the total binding. In all cases, the difference between total and nonspecific binding was statistically significant ($P < 0.05$; unpaired Student's *t*-test).

Interaction between CRLR and RAMP1. Since the discovery of RAMPs and their involvement in CRLR signaling, only scant attention has been paid to the interactions involving the different partners of the CRLR−RAMP complex. Cross-linking of [^{125}I]CGRP to two proteins with the molecular weight of CRLR plus RAMP1 and co-

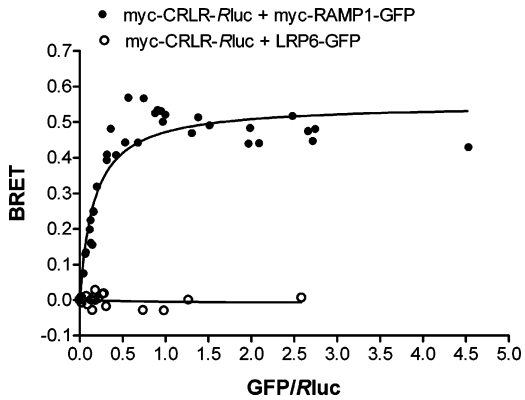

FIGURE 3: Interaction between CRLR and RAMP1 assessed by BRET. BRET titration curves were obtained using cells transfected with a constant amount of myc-CRLR-*R*luc and an increasing amount of either myc-RAMP1-GFP or LRP6-GFP. BRET values are plotted as a function of the ratio of total GFP over *R*luc expression obtained by measuring the total fluorescence and luminescence under each condition. Data points obtained in three to four independent experiments were pooled and used to generate the curves.

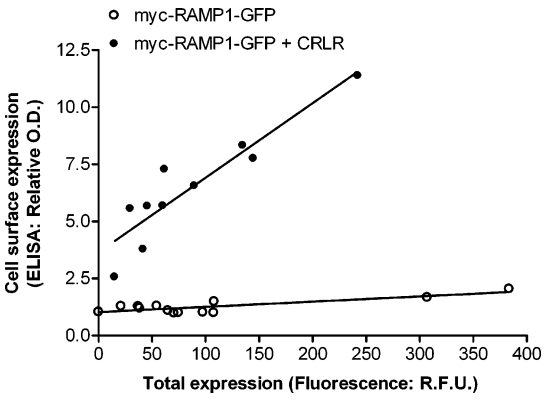

FIGURE 4: Cell surface targeting of RAMP1. HEK293T cells were transfected with an increasing amount of myc-RAMP1-GFP alone or in combination with a fixed amount of CRLR. Cell surface expression of myc-RAMP1-GFP was assessed by ELISA detection of the myc epitope and correlated with its total expression level determined by measuring the GFP fluorescence. Data points obtained in three independent experiments were pooled and used to generate the curves.

immunoprecipitation of CRLR and RAMP1 after cell solubilization suggested an interaction between CRLR and RAMPs (*1*−*11*). To determine whether such interaction occurred in vivo, BRET titration curves were carried out in living cells. For this purpose, a constant level of myc-CRLR-*R*luc was coexpressed with increasing concentrations of myc-RAMP1-GFP in HEK293T cells. As shown in Figure 3, the magnitude of the BRET signal detected in cells expressing the two constructs increased as a hyperbolic function of the myc-RAMP1-GFP concentration, reflecting a specific interaction between the two proteins (*18*). Similar results were obtained when the reverse energy donor−acceptor orientation was used (coexpressing myc-RAMP1-*R*luc with myc-CRLR-GFP; Figure S2A of the Supporting Information). In contrast, virtually no BRET signal could be detected between myc-CRLR-*R*luc and the negative control LRP6-GFP [a single-transmembrane domain coreceptor for another 7TMR, Frizzled (Fz) (*23*)] expressed at levels similar to those of myc-RAMP1-GFP (as illustrated by the similar fluorescence obtained in cells transfected with either LRP6-GFP or myc-RAMP1-GFP), thus confirming the selectivity of the observed signal. The addition of CGRP to cells coexpressing myc-CRLR-*R*luc and myc-RAMP1-GFP was without effect on the BRET signal (data not shown), indicating that agonist stimulation did not affect the oligomeric state of the complex. To rule out the possibility that the lack of an effect of CGRP on the BRET between myc-CRLR-*R*luc and myc-RAMP1-GFP could result from the presence of a significant pool of intracellular CRLR−RAMP1 complex that could not be accessible to CGRP, the effect of CGRP was assessed on membrane fractions derived from cells coexpressing myc-CRLR-*R*luc and myc-RAMP1-GFP. As shown in Figure S2B of the Supporting Information, CGRP, at a saturating concentration of 1 μM, was without effect on the BRET signal between CRLR and RAMP1. Taken together, these results clearly indicate that, as suggested by in vitro studies, CRLR and RAMP1 can form a constitutive and stable complex in living cells.

It has previously been demonstrated that the single substitution of any of the four conserved cysteine residues in the N-terminal domain of RAMP1 with alanine residues impaired the CGRP receptor function by promoting retention of the mutated RAMP1, even when coexpressed with CRLR (*24*). This retention could be explained by different mechanisms, one being that the cysteine mutation could impair the physical interaction between RAMP1 and CRLR, which is needed for cell surface trafficking. To test this hypothesis, we constructed a myc-RAMP1C104A-GFP mutant and tested both its subcellular localization and its ability to interact with CRLR.

To quantitatively assess the cell surface targeting of myc-RAMP1-GFP, we devised an assay based on the simultaneous measurement of the surface expression by an ELISA (using the N-terminal myc epitope) and of the total myc-RAMP1-GFP expression, reflected by the fluorescence of the C-terminally fused GFP. The cell surface expression (ELISA signal) is then graphically depicted as a function of the total expression level (fluorescence). As shown in Figure 4, expressing increasing levels of myc-RAMP1-GFP in the absence of CRLR led to a robust elevation of the fluorescence that was detected, but to virtually no increase in the magnitude of the ELISA signal, confirming that RAMP1 cannot reach the cell surface efficiently in the absence of CRLR. At similar fluorescence levels of myc-RAMP1-GFP, coexpression of CRLR promoted a brisk increase in the magnitude of the ELISA signal that is proportional to its total level of expression, reflecting the ability of the complex to reach the cell surface. In contrast, no cell surface signal could be observed for the myc-RAMP1C104A-GFP mutant even in the presence of CRLR (Figure 5A), confirming the intracellular retention phenotype of that cysteine-mutated RAMP1 (*24*).

To assess the ability of RAMP1C104A to interact with CRLR, BRET titration curves were carried out with myc-CRLR-*R*luc and either myc-RAMP1-GFP, myc-RAMP1C104A-GFP, or LRP6-GFP (Figure 5B). A hyperbolic increase in the magnitude of the BRET signal was observed for both myc-RAMP1-GFP and myc-RAMP1C104A-GFP but not LRP6-GFP, indicating that the cysteine mutation did not prevent the interaction between RAMP1 and CRLR. The observation that similar levels of RAMP1 expression were required for myc-RAMP1-GFP and myc-RAMP1C104A-

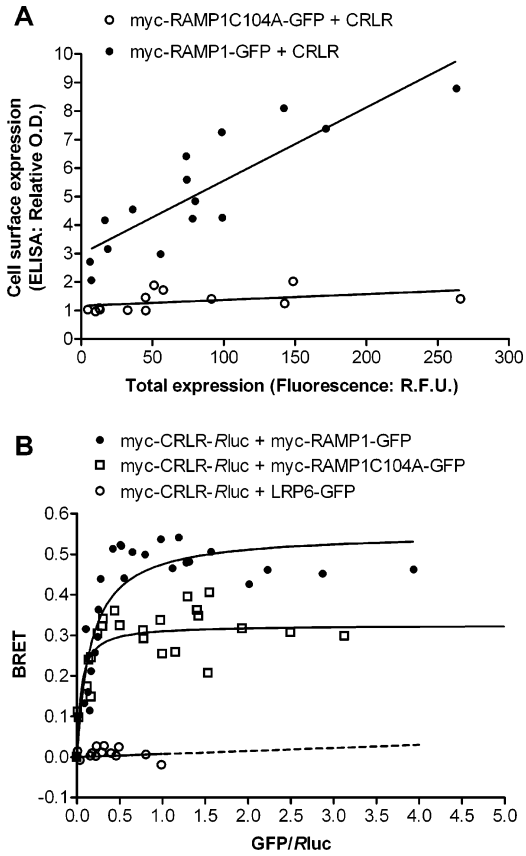

FIGURE 5: RAMP1C104A cell surface targeting and interaction with CRLR. (A) HEK293T cells were transfected with a fixed amount of CRLR and increasing amounts of either myc-RAMP1-GFP or myc-RAMP1C104A-GFP. Cell surface expression of the RAMP1 constructs was assessed by ELISA detection of the myc epitope and correlated with their total expression levels by measuring the GFP fluorescence. (B) BRET titration curves were obtained using cells transfected with a constant amount of myc-CRLR-*R*luc and an increasing amount of either myc-RAMP1-GFP, myc-RAMP1C104A-GFP, or LRP6-GFP. BRET values are plotted as a function of the ratio of total GFP over *R*luc expression obtained by measuring the total fluorescence and luminescence under each condition. The $BRET_{max}$ and $BRET_{50}$ values were derived from nonlinear least-squares regressions curve fitting (GraphPad Prism). $BRET_{max} = 0.55 \pm 0.03$ for myc-RAMP1-GFP and 0.32 ± 0.02 for myc-RAMP1C104A-GFP. $BRET_{50} = 0.16 \pm 0.04$ for myc-RAMP1-GFP and 0.05 ± 0.02 for myc-RAMP1C104A-GFP. Data points obtained in three independent experiments were pooled and used to generate the curves.

GFP to reach 50% of the maximal BRET signal [termed $BRET_{50}$ values and used as an indirect indication of the relative affinity of the partners for one another (*18*)] indicates that the mutation did not inhibit the ability of RAMP1 to associate with CRLR. In fact, the modestly smaller $BRET_{50}$ observed for myc-RAMP1C104A-GFP suggests that the mutant form of RAMP1 may even have a slightly greater affinity for CRLR. The maximal BRET signal observed was, however, markedly smaller for the mutant form of RAMP1. Maximal BRET levels reflect not only the number of dimers but also the distance and orientation between the energy donors and acceptors that can be affected by conformational changes. Given the lack of a $BRET_{50}$ increase, which indicates a similar propensity of the mutant and WT RAMP1 to associate with CRLR, the smaller $BRET_{max}$ most likely reflects a conformational difference between the CRLR−RAMP1C104A and CRLR−RAMP1 complexes. It follows that the intracellular retention of the cysteine mutant is probably due to a distinct conformation of the CRLR−RAMP1C104A complex that does not allow its export from the ER. This conformational change could result from the inability of RAMP1 to form intra- or intermolecular disulfide bonds involving cysteine 104 (*6*). Alternatively, the decrease in $BRET_{max}$ could reflect a retention of the myc-RAMP1C104A-GFP in a subcellular compartment where it can interact only with a fraction of the myc-CRLR-*R*luc population. However, such hypothetical partial sequestration of the mutated RAMP1 away from CRLR could not explain the total intracellular retention of RAMP1C104A (Figure 5A). Indeed, the extent of the BRET signal observed with myc-RAMP1C104A-GFP indicates that a sizable fraction of the mutated RAMP1 can interact with CRLR but cannot reach the cell surface.

Homodimerization of CRLR. A growing body of data suggests that most members of the GPCR superfamily can form dimers. Although most attention focused on family A and C receptors, a growing body of evidence suggests that family B GPCRs such as the calcitonin (*25*), corticotropin-releasing factor receptor type 1 (*26*), secretin (*27*), and vasoactive intestinal polypeptide/pituitary adenylate cyclase-activating peptide (VPAC1 and VPAC2) (*28*) receptors can also form dimers. Several of these receptors have also been shown to interact with RAMPs (*12*, *13*). However, CRLR is a special case since it is the only receptor to date that absolutely requires RAMPs for its plasma membrane expression, function, and pharmacological selectivity. Since GPCR homo- and heterodimerization have also been shown to play a role in receptor cell surface trafficking (*29*, *30*), we sought to assess whether CRLR could also homodimerize in living cells. For this purpose, BRET titration experiments, where a constant level of myc-CRLR-*R*luc was coexpressed with increasing concentrations of myc-CRLR-GFP, were carried out. As shown in Figure 6A, the magnitude of the BRET signal increased as a hyperbolic function of the concentration of GFP fusion protein added, whereas coexpression of myc-CRLR-*R*luc with an unrelated 7TMR Fz1 fused to GFP (Fz1-GFP) led only to marginal BRET that increased linearly as a function of GFP concentration. The weak and linear signal observed between myc-CRLR-*R*luc and Fz1-GFP most likely represents "bystander BRET" resulting from random collisions between the expressed BRET partners (*18*), thus emphasizing the fact that the robust hyperbolic signal detected for the myc-CRLR-*R*luc−myc-CRLR-GFP pair reflects selective dimerization of CRLR. To confirm the occurrence of homodimerization using a different approach, co-immunoprecipitation experiments were carried out in solubilized preparations derived from cells coexpressing differentially amino-terminally tagged CRLR. As shown in Figure 6B (lane 3), immunoreactivity corresponding to the myc-tagged CRLR could be readily detected following immunoprecipitation of the HA-CRLR, indicating an intermolecular interaction between the differentially tagged receptor that is consistent with the CRLR homodimerization detected by BRET. No myc immunoreactivity was detected following immunoprecipitation with the anti-HA antibody in cells expressing either myc-CRLR or HA-CRLR alone (Figure 6B, lanes 1 and 2), demonstrating that the signal did not result from cross-immunoreactivity. In cells coexpressing myc-CRLR and HA-Fz1, immunoprecipitation of

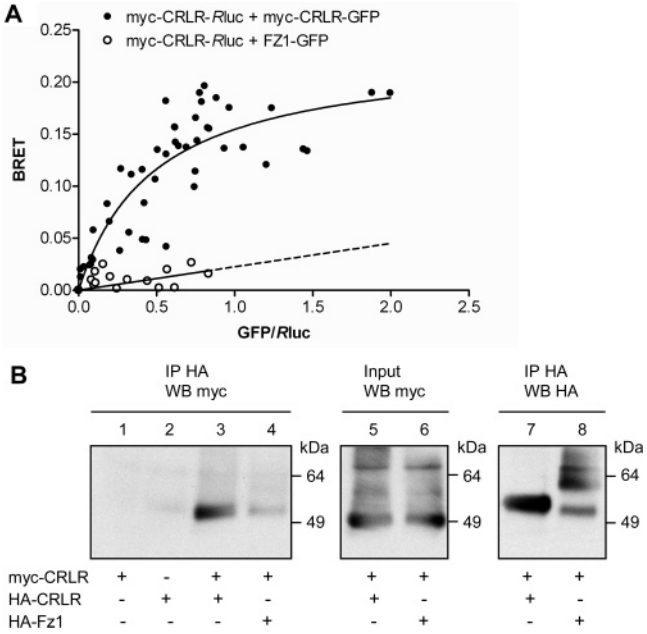

FIGURE 6: Homodimerization of CRLR. (A) BRET titration curves were obtained using cells transfected with a constant amount of myc-CRLR-*R*luc and an increasing amount of either myc-CRLR-GFP or Fz1-GFP. BRET values are plotted as a function of the ratio of total GFP over *R*luc expression obtained by measuring the total fluorescence and luminescence under each condition. Data points obtained in four to nine independent experiments were pooled and used to generate the curves. (B) HA-tagged receptors were immunoprecipitated from cells transfected with the indicated constructs, and the myc-associated (lanes 1−4) and HA-associated (lanes 7 and 8) immunoreactivities were revealed by Western blot analysis. The presence of myc-CRLR in cell extracts was also revealed by Western blot analysis (lanes 5 and 6). The results shown are representative of three independent experiments.

HA-Fz1 also led to a detectable cosedimentation of myc-CRLR (Figure 6B, lane 4). However, the myc-CRLR immunoreactivity that was detected was much weaker than that observed following HA-CRLR immunoprecipitation, despite equivalent levels of myc-CRLR (Figure 6B, lanes 5 and 6) and the similar amount of HA-tagged receptors that immunoprecipitated (Figure 6B, lanes 7 and 8). The low level of co-immunoprecipitation between CRLR and Fz1 most likely represents nonspecific interactions that are consistent with the weak BRET signal observed between myc-CRLR-*R*luc and Fz1-GFP in Figure 6A. Taken together, the BRET and co-immunoprecipitation data demonstrate for the first time that even though it requires a coreceptor for cell surface trafficking and function, CRLR has the same homo-oligomerization potential as the other GPCRs.

Homo- and Heterodimerization of RAMP1. Even if the evidence is less compelling than that for GPCRs, RAMP1 has also been proposed to form homodimers. For instance, species corresponding to the expected molecular weight for a dimer of RAMP1 were obtained following immunoprecipitation of an N-terminally tagged RAMP1 (*1*, *6*, *16*, *17*). Although this could indeed reflect RAMP1 homodimerization, the detection of a higher-molecular weight species could also be a consequence of the association of RAMP1 with another protein with a similar molecular weight, or of aggregation resulting from cell lysis and incomplete solubilization. To directly assess if RAMP1 could truly form homodimers in living cells, BRET titration experiments were carried out. A robust and saturable transfer of energy was

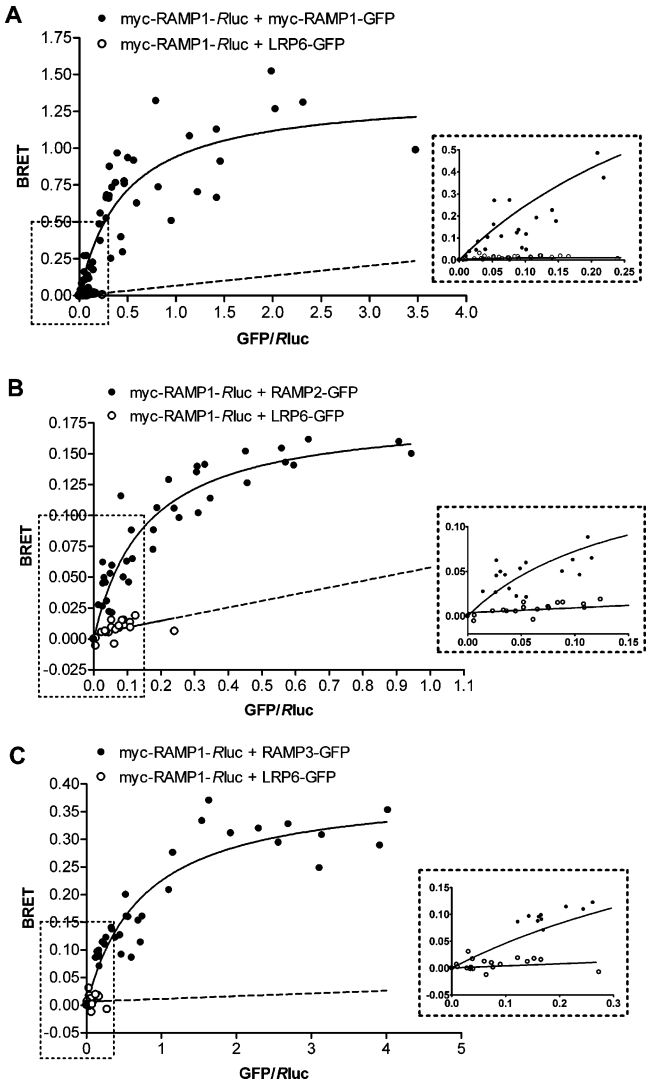

FIGURE 7: Homo- and heterodimerization of RAMP1. BRET titration curves were obtained using cells transfected with a constant amount of myc-RAMP1-*R*luc and an increasing amount of either myc-RAMP1-GFP (A), RAMP2-GFP (B), RAMP3-GFP (C), or LRP6-GFP (A−C). BRET values are plotted as a function of the ratio of total GFP over *R*luc expression obtained by measuring the total fluorescence and luminescence under each condition. The inset corresponds to the enlargement of the region delineated by the dotted line. Data points obtained in four to nine independent experiments were pooled and used to generate the curves.

obtained between myc-RAMP1-*R*luc and myc-RAMP1-GFP (Figure 7A). As in the case of the CRLR−RAMP1 interaction, LRP6-GFP was used as a negative control. In spite of the low expression levels of the negative control, it can be clearly seen that coexpression of myc-RAMP1-*R*luc with LRP6-GFP led to undetectable BRET signals at GFP/*R*luc ratios for which sizable BRET levels were obtained between RAMP1-*R*luc and RAMP1-GFP (inset of Figure 7A), thus confirming the selectivity of the observed signal. The negative results obtained with Fz1-GFP (Figure 6A) and LRP6-GFP (Figures 3 and 7A) do not result from the inability of these constructs to generate BRET signals, since significant BRET levels were obtained when Fz1-*R*luc was coexpressed with Fz1-GFP and LRP6-*R*luc with LRP6-GFP (Figure S3 of the Supporting Information). Taken together, these data provide the first evidence that RAMP1 can form homodimers in intact living cells. Given the existence of three

RAMP subtypes, we investigated the ability of RAMP1 to heterodimerize with the two other members of the family, RAMP2 and RAMP3. For this purpose, RAMP2 and RAMP3 fused at their carboxyl termini to GFP were used as potential BRET partners for myc-RAMP1-*R*luc. As was the case for RAMP1, the addition of GFP to RAMP2 and RAMP3 did not affect the functional properties of these proteins as assessed by their ability to confer [^{125}I]AM binding (data not shown). BRET titration curves revealed that RAMP1 readily interacts with both RAMP2 and RAMP3, as indicated by the fact that the magnitude of the BRET signal observed between myc-RAMP1-*R*luc and either RAMP2- or RAMP3-GFP increased as a hyperbolic function of the GFP partner concentration (panel B or C of Figure 7, respectively). The selectivity of the interaction was once again confirmed by the lack of BRET between myc-RAMP1-*R*luc and LRP6-GFP. These data reveal that, in addition to self-association, RAMP1 can also interact with the two other members of the family to form heterodimers.

Effects of RAMP1 Dimerization on Cell Surface Targeting of RAMP1Δ8. To further asses the functional relevance of RAMP1 dimerization, we took advantage of a truncated form of RAMP1 (RAMP1Δ8), which exhibits receptor-independent cell surface delivery as a result of the deletion of a retention signal (SKRT) located within its last eight amino acids (*4*). Indeed, as discussed before, the WT form of RAMP1 is retained intracellularly when expressed alone. If, as the BRET experiments described above indicate, RAMP1 can homodimerize, coexpression of RAMP1Δ8 with WT RAMP1 could have an impact on their cell surface expression. Either RAMP1Δ8 could bring its WT counterpart to the cell surface, or WT RAMP1 could retain the truncated form intracellularly.

Before these possibilities were tested, the functionality of myc-RAMP1Δ8-GFP, its cell surface trafficking property, and its ability to dimerize with WT RAMP1 were assessed. As seen in Table 1, similar to WT RAMP1, coexpression of myc-RAMP1Δ8-GFP with CRLR conferred high-affinity [^{125}I]CGRP binding, confirming the functional status of the truncated form of RAMP1 (*4*). Using the quantitative cell surface targeting assay described above, the plasma membrane expression profile of myc-RAMP1Δ8-GFP was compared to that of myc-RAMP1-GFP. As shown in Figure 8A, in contrast to full-length myc-RAMP1-GFP, an increasing level of expression of truncated RAMP1 alone led to the apparition of detectable cell surface RAMP1 expression, confirming the CRLR-independent cell surface delivery of myc-RAMP1Δ8-GFP. Finally, the ability of RAMP1Δ8 to dimerize with WT RAMP1 was confirmed by the strong BRET signal observed upon coexpression of myc-RAMP1Δ8-GFP with HA-RAMP1-*R*luc (Figure 8B).

To assess the potential influence of dimerization on RAMP cell surface trafficking, we then proceeded to measure the influence of HA-RAMP1-*R*luc on the cell surface delivery of myc-RAMP1Δ8-GFP. As seen in Figure 9, coexpression of an excess of HA-RAMP1-*R*luc prevented the cell surface appearance of myc-RAMP1Δ8-GFP for a wide range of truncated RAMP1 expression levels. The intracellular retention of myc-RAMP1Δ8-GFP was dependent on the amount of HA-RAMP1-*R*luc expressed, since titrating down its expression resulted in weaker retention (data not shown). Taken together, these results indicate that full-length RAMP1

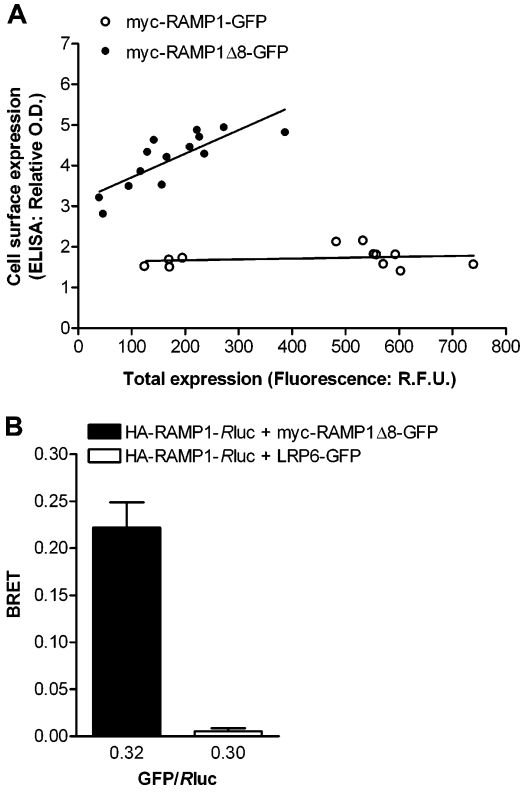

FIGURE 8: Cell surface targeting and dimerization of RAMP1Δ8. (A) HEK293T cells were transfected with an increasing amount of myc-RAMP1-GFP or myc-RAMP1Δ8-GFP. Cell surface expression of these proteins was assessed by ELISA detection of the myc epitope and correlated with their total expression level determined by measuring the total fluorescence of GFP. Data points obtained in two independent experiments were pooled and used to generate the curves. (B) BRET values, as well as total fluorescence and luminescence levels, were measured in cells expressing HA-RAMP1-*R*luc in combination with either myc-RAMP1Δ8-GFP or LRP6-GFP. The total fluorescence/luminescence ratios for each condition are given under the bars corresponding to the BRET values. The data represent the mean ± standard error of the mean of three to four independent experiments.

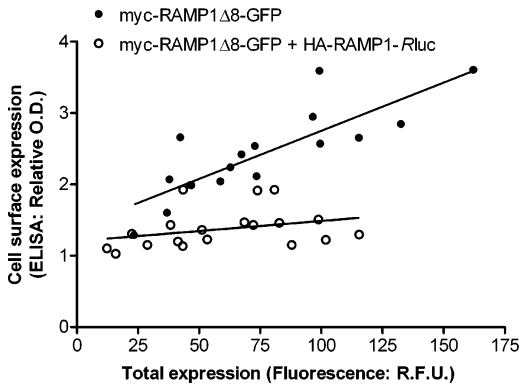

FIGURE 9: Influence of WT RAMP1 coexpresssion on RAMP1Δ8 cell surface targeting. HEK293T cells were transfected with an increasing amount of myc-RAMP1Δ8-GFP alone or in combination with a fixed amount of HA-RAMP1-*R*luc. Cell surface expression of myc-RAMP1Δ8-GFP was assessed by ELISA detection of the myc epitope and correlated with its total expression level by measuring the total fluorescence from the GFP. Data points obtained in three independent experiments were pooled and used to generate the curves.

acts as a dominant negative of RAMP1Δ8 cell surface targeting, suggesting that the dimerization occurs intracellularly, most likely in the ER or the Golgi, where it could

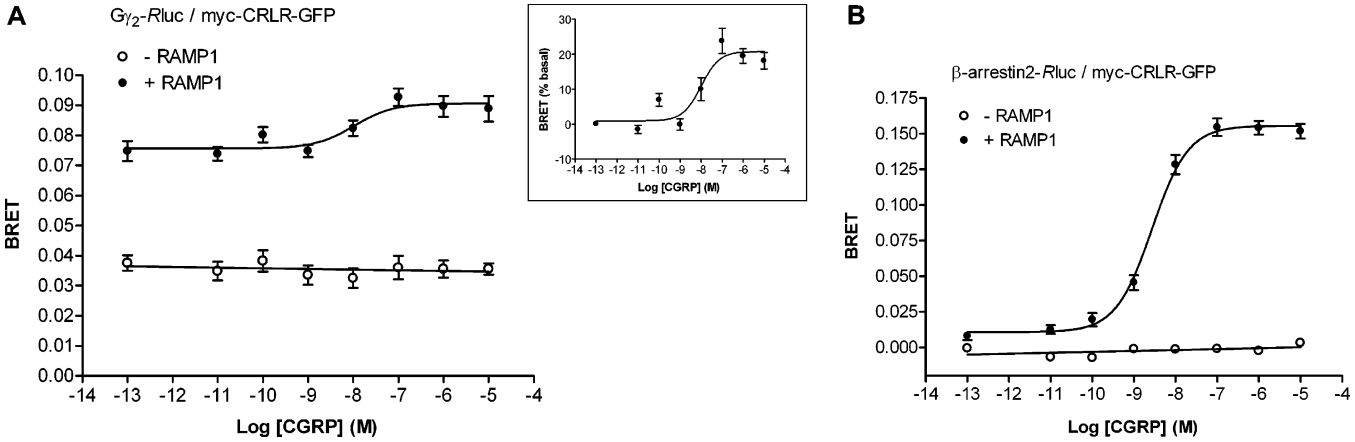

FIGURE 10: CRLR−RAMP1 signaling complexes assessed by BRET. HEK293T cells were transfected with myc-CRLR-GFP and either the Gγ_2-*R*luc, Gβ_1, and Gα_s complex (A) or β-arrestin2-*R*luc (B). The BRET values were determined in the absence (−RAMP1) or presence (+RAMP1) of cotransfected RAMP1, 10 min after stimulation with different concentrations of CGRP. GFP and *R*luc fusion protein expression levels were controlled by measuring the total fluorescence and luminescence, and were found to be similar in the presence and absence of cotransfected RAMP1. The inset in panel A illustrates the agonist-promoted increase in the magnitude of the BRET signal expressed as a percentage of the basal BRET value obtained in the absence of ligand. The EC_{50} values derived from these curves are 16.1 ± 13.4 nM for the Gγ_2-*R*luc−myc-CRLR-GFP pair and 2.8 ± 0.5 nM for the β-arrestin2-*R*luc−myc-CRLR-GFP pair, both in the presence of RAMP1. The data shown represent the mean ± standard error of the mean of three independent experiments.

play a role in the processing of RAMP1 through the secretory pathway. Such dimerization early in the secretory pathway is reminiscent of the oligomerization of two lectin proteins, ERGIC-53 and VIP36, that share a similar topological organization with RAMP1 (type I single-transmembrane protein) and are involved in ER−Golgi transport of glycoproteins (*31*, *32*). Interestingly, the oligomerization of ERGIG-53 was found to be essential for its cargo transport function (*33*). However, the role of RAMP1 dimerization in the transport of the CRLR−RAMP1 complex remains to be investigated.

CRLR−RAMP1 Signaling Complexes Assessed by BRET. Binding of CGRP to its receptor (presumably the CRLR−RAMP1 complex) leads to the activation of the stimulatory G protein (Gs) that in turns activates adenylyl cyclase activity, promoting the appropriate cellular responses (*34*). In addition to its coupling to Gs, the CRLR−RAMP1 complex has also been proposed to interact with β-arrestin (*6*), an accessory protein that promotes the desensitization and internalization of GPCRs and may lead to the activation of the mitogen-activated protein kinase pathway (*35*). However, the evidence linking CRLR itself to G proteins and β-arrestin is only indirect. Thus, we turned to BRET assays to probe the direct interaction between CRLR and its signaling partners, and tested the role of RAMP1 in such interactions. For the G protein coupling, the energy transfer between Gγ_2-*R*luc and myc-CRLR-GFP was monitored in the presence or absence of cotransfected RAMP1. In all cases, the BRET partners were coexpressed with Gα_s and Gβ_1 to attain the G protein subunit stoichiometry needed to allow the proper engagement of the heterotrimeric G proteins by the receptor (*19*). As illustrated in Figure 10A, stimulation with CGRP led to a concentration-dependent increase in the magnitude of the BRET signal detected only in cells transfected with RAMP1. Interestingly, the expression of RAMP1 was sufficient to noticeably increase the magnitude of the basal BRET signal between CRLR and Gγ, indicating that RAMP1 favors constitutive coupling between the 7TMR and the G protein. The existence of such precoupling between GPCRs and their cognate G proteins has been previously suggested (*36*) and recently confirmed for several receptors, using both BRET (*19*) and FRET (fluorescence resonance energy transfer) (*37*) approaches. Taken together, these data demonstrate the necessity of RAMP1 for proper engagement of G proteins by CRLR. The data are also consistent with the notion that the CRLR−RAMP1 complex represents the functional receptor interacting with the G protein upon agonist stimulation, yet one cannot exclude the possibility that, although necessary for the trafficking of CRLR at the plasma membrane, RAMP1 could dissociate from the receptor once at the cell surface, thus allowing CRLR to interact on its own with the G protein. However, this possibility is unlikely since it was previously shown that CGRP can be chemically cross-linked to both CRLR and RAMP1 and that agonist stimulation leads to the endocytosis of the CRLR−RAMP1 complex as a stable entity, suggesting that CRLR and RAMP1 remain associated following agonist binding and activation (*6*, *11*).

In the case of β-arrestin, the agonist-promoted recruitment was monitored in cells coexpressing β-arrestin2-*R*luc and myc-CRLR-GFP. No detectable basal BRET was observed regardless of whether RAMP1 was cotransfected (Figure 10B), consistent with the notion that under resting conditions, β-arrestin resides in the cytosol and thus does not interact with either ER-retained or plasma membrane-targeted receptors. Following CGRP stimulation, a robust concentration-dependent increase in the extent of energy transfer between β-arrestin2-*R*luc and myc-CRLR-GFP was observed only in cells transfected with RAMP1, thus confirming that CRLR can recruit β-arrestin upon activation exclusively in the context of RAMP1 coexpression. These results are congruent with the observation that CRLR and RAMP1 undergo β-arrestin-dependent endocytosis as a stable complex following receptor activation (*6*). It is noteworthy that the apparent potency (EC_{50}) of the CGRP-promoted interaction of CRLR with both Gγ and β-arrestin monitored by BRET (Figure 10A,B) was similar to the apparent affinity (IC_{50}) of the receptor as assessed in a CGRP radioligand competition binding assay (Table 1). However, the apparent potency obtained in the BRET assays is significantly lower than that

observed for the CGRP-stimulated cAMP production (Figure 2A). This difference is not surprising when one considers that the second-messenger generation greatly amplifies the signal, thus unmasking the presence of spare receptors that leads to a leftward shift in the concentration−response curve.

Overall, our results are in agreement with the notion that the CRLR−RAMP1 complex represents the functional CGRP receptor (*1*) and demonstrate for the first time that such physical assembly occurs in living cells. They also clearly demonstrate that, in the context of RAMP1 coexpression, CRLR can engage both the G proteins and β-arrestin, confirming its signaling capacities. In addition to their ability to interact with one another, CRLR and RAMP1 were also found to form homodimers in living cells, thus raising the question of their stoichiometry of assembly in the CRLR−RAMP1 complex. Unfortunately, the assays currently available do not allow us to readily address this question in intact cells, and further methodological development will be needed before a satisfactory answer to this question can be offered. Despite this limitation, the BRET assays presented in this study offer new ways of probing CGRP receptor assembly and activity.

ACKNOWLEDGMENT

We are grateful to Dr. S. M. Foord (GlaxoSmithKline) for the generous gift of CRLR, RAMP1, myc-CRLR, and myc-RAMP1, Dr. P. M. Sexton for RAMP2-GFP and RAMP3-GFP, and Dr. R. T. Moon for Fz1-GFP and LRP6-GFP cDNAs. We also thank Dr. M. Lagacé for critical reading of the manuscript.

SUPPORTING INFORMATION AVAILABLE

Cell surface trafficking of myc-CRLR (Figure S1), BRET between myc-RAMP1-*R*luc and myc-CRLR-GFP (Figure S2A), effect of CGRP on the BRET between myc-CRLR-*R*luc and myc-RAMP1-GFP (Figure S2B), and BRET between LRP6-*R*luc and LRP6-GFP and between Fz1-*R*luc and Fz1-GFP (Figure S3). This material is available free of charge via the Internet at http://pubs.acs.org.

REFERENCES

1. McLatchie, L. M., Fraser, N. J., Main, M. J., Wise, A., Brown, J., Thompson, N., Solari, R., Lee, M. G., and Foord, S. M. (1998) RAMPs regulate the transport and ligand specificity of the calcitonin-receptor-like receptor, *Nature 393*, 333−339.
2. Leuthauser, K., Gujer, R., Aldecoa, A., McKinney, R. A., Muff, R., Fischer, J. A., and Born, W. (2000) Receptor-activity-modifying protein 1 forms heterodimers with two G-protein-coupled receptors to define ligand recognition, *Biochem. J. 351* (Part 2), 347−351.
3. Gujer, R., Aldecoa, A., Buhlmann, N., Leuthauser, K., Muff, R., Fischer, J. A., and Born, W. (2001) Mutations of the asparagine 117 residue of a receptor activity-modifying protein 1-dependent human calcitonin gene-related peptide receptor result in selective loss of function, *Biochemistry 40*, 5392−5398.
4. Steiner, S., Muff, R., Gujer, R., Fischer, J. A., and Born, W. (2002) The transmembrane domain of receptor-activity-modifying protein 1 is essential for the functional expression of a calcitonin gene-related peptide receptor, *Biochemistry 41*, 11398−11404.
5. Flahaut, M., Rossier, B. C., and Firsov, D. (2002) Respective roles of calcitonin receptor-like receptor (CRLR) and receptor activity-modifying proteins (RAMP) in cell surface expression of CRLR/RAMP heterodimeric receptors, *J. Biol. Chem. 277*, 14731−14737.
6. Hilairet, S., Belanger, C., Bertrand, J., Laperriere, A., Foord, S. M., and Bouvier, M. (2001) Agonist-promoted internalization of a ternary complex between calcitonin receptor-like receptor, receptor activity-modifying protein 1 (RAMP1), and β-arrestin, *J. Biol. Chem. 276*, 42182−42190.
7. Koller, D., Ittner, L. M., Muff, R., Husmann, K., Fischer, J. A., and Born, W. (2004) Selective inactivation of adrenomedullin over calcitonin gene-related peptide receptor function by the deletion of amino acids 14−20 of the mouse calcitonin-like receptor, *J. Biol. Chem. 279*, 20387−20391.
8. Ittner, L. M., Luessi, F., Koller, D., Born, W., Fischer, J. A., and Muff, R. (2004) Aspartate(69) of the calcitonin-like receptor is required for its functional expression together with receptor-activity-modifying proteins 1 and -2, *Biochem. Biophys. Res. Commun. 319*, 1203−1209.
9. Ittner, L. M., Koller, D., Muff, R., Fischer, J. A., and Born, W. (2005) The N-terminal extracellular domain 23−60 of the calcitonin receptor-like receptor in chimeras with the parathyroid hormone receptor mediates association with receptor activity-modifying protein 1, *Biochemistry 44*, 5749−5754.
10. Koller, D., Born, W., Leuthauser, K., Fluhmann, B., McKinney, R. A., Fischer, J. A., and Muff, R. (2002) The extreme N-terminus of the calcitonin-like receptor contributes to the selective interaction with adrenomedullin or calcitonin gene-related peptide, *FEBS Lett. 531*, 464−468.
11. Hilairet, S., Foord, S. M., Marshall, F. H., and Bouvier, M. (2001) Protein-protein interaction and not glycosylation determines the binding selectivity of heterodimers between the calcitonin receptor-like receptor and the receptor activity-modifying proteins, *J. Biol. Chem. 276*, 29575−29581.
12. Christopoulos, G., Perry, K. J., Morfis, M., Tilakaratne, N., Gao, Y., Fraser, N. J., Main, M. J., Foord, S. M., and Sexton, P. M. (1999) Multiple amylin receptors arise from receptor activity-modifying protein interaction with the calcitonin receptor gene product, *Mol. Pharmacol. 56*, 235−242.
13. Christopoulos, A., Christopoulos, G., Morfis, M., Udawela, M., Laburthe, M., Couvineau, A., Kuwasako, K., Tilakaratne, N., and Sexton, P. M. (2003) Novel receptor partners and function of receptor activity-modifying proteins, *J. Biol. Chem. 278*, 3293−3297.
14. Bouschet, T., Martin, S., and Henley, J. M. (2005) Receptor-activity-modifying proteins are required for forward trafficking of the calcium-sensing receptor to the plasma membrane, *J. Cell Sci. 118*, 4709−4720.
15. Terrillon, S., and Bouvier, M. (2004) Roles of G-protein-coupled receptor dimerization, *EMBO Rep. 5*, 30−34.
16. Sexton, P. M., Albiston, A., Morfis, M., and Tilakaratne, N. (2001) Receptor activity modifying proteins, *Cell. Signalling 13*, 73−83.
17. Udawela, M., Hay, D. L., and Sexton, P. M. (2004) The receptor activity modifying protein family of G protein coupled receptor accessory proteins, *Semin. Cell Dev. Biol. 15*, 299−308.
18. Mercier, J. F., Salahpour, A., Angers, S., Breit, A., and Bouvier, M. (2002) Quantitative assessment of β1- and β2-adrenergic receptor homo- and heterodimerization by bioluminescence resonance energy transfer, *J. Biol. Chem. 277*, 44925−44931.
19. Gales, C., Rebois, R. V., Hogue, M., Trieu, P., Breit, A., Hebert, T. E., and Bouvier, M. (2005) Real-time monitoring of receptor and G-protein interactions in living cells, *Nat. Methods 2*, 177−184.
20. Charest, P. G., and Bouvier, M. (2003) Palmitoylation of the V2 vasopressin receptor carboxyl tail enhances β-arrestin recruitment leading to efficient receptor endocytosis and ERK1/2 activation, *J. Biol. Chem. 278*, 41541−41551.
21. Mellon, P., Parker, V., Gluzman, Y., and Maniatis, T. (1981) Identification of DNA sequences required for transcription of the human α1-globin gene in a new SV40 host-vector system, *Cell 27*, 279−288.
22. Durocher, Y., Perret, S., and Kamen, A. (2002) High-level and high-throughput recombinant protein production by transient transfection of suspension-growing human 293-EBNA1 cells, *Nucleic Acids Res. 30*, E9.
23. Tamai, K., Semenov, M., Kato, Y., Spokony, R., Liu, C., Katsuyama, Y., Hess, F., Saint-Jeannet, J. P., and He, X. (2000) LDL-receptor-related proteins in Wnt signal transduction, *Nature 407*, 530−535.

24. Steiner, S., Born, W., Fischer, J. A., and Muff, R. (2003) The function of conserved cysteine residues in the extracellular domain of human receptor-activity-modifying protein, *FEBS Lett. 555*, 285−290.
25. Seck, T., Baron, R., and Horne, W. C. (2003) The alternatively spliced Δe13 transcript of the rabbit calcitonin receptor dimerizes with the C1a isoform and inhibits its surface expression, *J. Biol. Chem. 278*, 23085−23093.
26. Kraetke, O., Wiesner, B., Eichhorst, J., Furkert, J., Bienert, M., and Beyermann, M. (2005) Dimerization of corticotropin-releasing factor receptor type 1 is not coupled to ligand binding, *J. Recept. Signal Transduction Res. 25*, 251−276.
27. Ding, W. Q., Cheng, Z. J., McElhiney, J., Kuntz, S. M., and Miller, L. J. (2002) Silencing of secretin receptor function by dimerization with a misspliced variant secretin receptor in ductal pancreatic adenocarcinoma, *Cancer Res. 62*, 5223−5229.
28. Harikumar, K. G., Morfis, M. M., Lisenbee, C. S., Sexton, P. M., and Miller, L. J. (2006) Constitutive formation of oligomeric complexes between family B G protein-coupled vasoactive intestinal polypeptide and secretin receptors, *Mol. Pharmacol. 69*, 363−373.
29. Salahpour, A., Angers, S., Mercier, J. F., Lagace, M., Marullo, S., and Bouvier, M. (2004) Homodimerization of the β2-adrenergic receptor as a prerequisite for cell surface targeting, *J. Biol. Chem. 279*, 33390−33397.
30. Bulenger, S., Marullo, S., and Bouvier, M. (2005) Emerging role of homo- and heterodimerization in G-protein-coupled receptor biosynthesis and maturation, *Trends Pharmacol. Sci. 26*, 131−137.
31. Hauri, H. P., Kappeler, F., Andersson, H., and Appenzeller, C. (2000) ERGIC-53 and traffic in the secretory pathway, *J. Cell Sci. 113* (Part 4), 587−596.
32. Fiedler, K., Parton, R. G., Kellner, R., Etzold, T., and Simons, K. (1994) VIP36, a novel component of glycolipid rafts and exocytic carrier vesicles in epithelial cells, *EMBO J. 13*, 1729−1740.
33. Appenzeller, C., Andersson, H., Kappeler, F., and Hauri, H. P. (1999) The lectin ERGIC-53 is a cargo transport receptor for glycoproteins, *Nat. Cell Biol. 1*, 330−334.
34. Foord, S. M., and Marshall, F. H. (1999) RAMPs: Accessory proteins for seven transmembrane domain receptors, *Trends Pharmacol. Sci. 20*, 184−187.
35. Lefkowitz, R. J., and Shenoy, S. K. (2005) Transduction of receptor signals by β-arrestins, *Science 308*, 512−517.
36. Rebois, R. V., and Hebert, T. E. (2003) Protein complexes involved in heptahelical receptor-mediated signal transduction, *Recept. Channels 9*, 169−194.
37. Nobles, M., Benians, A., and Tinker, A. (2005) Heterotrimeric G proteins precouple with G protein-coupled receptors in living cells, *Proc. Natl. Acad. Sci. U.S.A. 102*, 18706−18711.

BI0622470